

Contribution from the Institut für Physikalische und Theoretische Chemie, Universität Regensburg, 8400 Regensburg, Federal Republic of Germany, and Institut für Anorganische Chemie, Universität Karlsruhe, 7500 Karlsruhe, Federal Republic of Germany

## Temperature, Magnetic Field, and High-Pressure Effects on the Optical Properties of Quasi-One-Dimensional Crystals: Ethylenediammonium Tetracyanoplatinate(II)

R. DILLINGER, G. GLIEMANN,\* H. P. PFLEGER, and K. KROGMANN

Received August 9, 1982

The optical properties (polarized absorption and emission) of enH<sub>2</sub>CP single crystals under variation of temperature (1.9 K ≤ T ≤ 295 K), hydrostatic pressure (1 atm ≤ P ≤ 32 kbar) and magnetic fields (0 ≤ H ≤ 5 T) are reported. An extremely large pressure-induced red shift of ~360 cm<sup>-1</sup>·kbar<sup>-1</sup> has been observed. When the magnetic field is raised from 0 to 5 T, the emission is blue shifted by 220 cm<sup>-1</sup> and the intensity increases by a factor of ~10.

### Introduction

Tetracyanoplatinates(II), M<sub>x</sub>[Pt(CN)<sub>4</sub>]<sub>n</sub>H<sub>2</sub>O (MCP), tend to crystallize in quasi-one-dimensional (1-D) structures in which the square-planar [Pt(CN)<sub>4</sub>]<sup>2-</sup> units are stacked in columns.<sup>1,2</sup> The cations and the waters of crystallization are found between the columns. The Pt-Pt distance *R* in the direction of the columnar *c* axis varies with the choice of the cations *M* and/or with the water of crystallization content, between 3.09 and ~3.7 Å. This intracolumnar distance is short compared to the separation from column to column, resulting in a strongly anisotropic interaction between the complex ions. The optical properties of the crystalline tetracyanoplatinates(II), which depend systematically on the intracolumnar distance *R*, have been studied in detail under variation of temperature,<sup>3-6</sup> hydrostatic pressure,<sup>3,7,8</sup> impurity concentration of [Ni(CN)<sub>4</sub>]<sup>2-</sup> and [Pd(CN)<sub>4</sub>]<sup>2-</sup>,<sup>9-11</sup> and recently, strong magnetic fields.<sup>12,13</sup> As a result of the magneto-optical investigations it was found that the crystals emit from three distinct levels, which can be classified within the *D*<sub>4h</sub>' symmetry of a single [Pt(CN)<sub>4</sub>]<sup>2-</sup> complex.

So far, MCP salts with alkali, alkaline-earth, and rare-earth cations have been measured. Since Pflieger and Krogmann<sup>14</sup> determined the structure of a similar salt with the organic ethylenediammonium (enH<sub>2</sub><sup>2+</sup>) cation, the opportunity was offered to study the effect on the electronic properties after substitution of an inorganic cation by a voluminous organic

one. Therefore, we have measured the polarized emission under variation of temperature, hydrostatic pressure, and magnetic field strength and, further, the temperature dependence of the polarized absorption.

Throughout this paper, the choice of crystal axes will make the Pt chain parallel to *c*, in order to be consistent with previous spectroscopic work; this definition differs, however, from that of the structure determination<sup>14</sup> by *a*(this work) = *b*(ref 14), *b* = *c*(ref 14), and *c* = *a*(ref 14).

### Experimental Section

Ethylenediammonium tetracyanoplatinate(II), enH<sub>2</sub>CP, was synthesized by the reaction described by Krogmann and Pflieger.<sup>14</sup> Slow evaporation of the solution yielded single crystals, which were purified by repeated recrystallization. The single crystals were needle-shaped with a hexagonal base showing a metallic violet reflection and a yellow-orange transparency. For absorption measurements sufficiently thin crystals (~20 μm) were obtained by evaporating a drop of an aqueous solution on a small quartz plate.

The apparatus and methods for studying the polarized absorption are described in ref 15, for the polarized-emission measurements in ref 16, for the pressure experiments in ref 7, and for the magnetic field studies in ref 12.

### Results

**Polarized Absorption.** Figure 1 shows the polarized absorption spectrum for enH<sub>2</sub>CP single crystals at *T* = 295 K and *T* = 10 K. The spectra were recorded with the electric field vector  $\vec{E}$  parallel and perpendicular to the columnar axis *c*,  $\vec{E} \parallel c$  and  $\vec{E} \perp c$ , respectively. Whereas the  $\vec{E} \perp c$  absorption is relatively weak, for the  $\vec{E} \parallel c$  polarization we can only identify the strongly increasing slope at the long-wavelength side.

When the temperature is lowered, for  $\vec{E} \perp c$  a considerable red shift of the peak energy and a decrease of the half-width is observed. As Figure 2 shows, the red shift between room temperature and *T* ≈ 50 K is approximately linear with *T* and amounts to about 1200 cm<sup>-1</sup>. Below *T* = 50 K the peak energy remains nearly independent of the temperature. The half-width decrease is accompanied by an increase of the extinction, so that the integral intensity has a constant value within the temperature range studied. Lowering of the temperature also shifts the flank of the  $\vec{E} \parallel c$  absorption to the red. Therein we see an indication of a red shift of the  $\vec{E} \parallel c$  maximum.

**Temperature Behavior of the Polarized Emission.** Figure 3 shows the polarized emission spectra for enH<sub>2</sub>CP single crystals with  $\vec{E} \parallel c$  and  $\vec{E} \perp c$  at *T* = 295 K and *T* = 1.9 K. The energy of the  $\vec{E} \perp c$  emission maximum vs. temperature is plotted in Figure 4. Between *T* = 295 K and *T* ≈ 50 K the emission maximum is shifted to the red by about 1200 cm<sup>-1</sup>. Further decrease of the temperature down to *T* = 7 K has no influence on the emission frequency, but in the low-

\* To whom correspondence should be addressed at the Universität Regensburg.

- (1) K. Krogmann, *Angew. Chem.*, **81**, 10 (1969); K. Krogmann and D. Stephan, *Z. Anorg. Allg. Chem.*, **362**, 290 (1968); J. S. Miller and A. J. Epstein, *Prog. Inorg. Chem.*, **20**, 1 (1976).
- (2) W. Holzapfel, H. Yersin, and G. Gliemann, *Z. Kristallogr.*, **157**, 47 (1981).
- (3) H. Yersin and G. Gliemann, *Ann. N.Y. Acad. Sci.*, **313**, 539 (1978).
- (4) W. Holzapfel, H. Yersin, G. Gliemann, and H. H. Otto, *Ber. Bunsenges. Phys. Chem.*, **82**, 207 (1978).
- (5) H. Yersin, G. Gliemann, and H. S. Råde, *Chem. Phys. Lett.*, **54**, 111 (1978).
- (6) W. Daniels, H. Yersin, H. v. Philipsborn, and G. Gliemann, *Solid State Commun.*, **30**, 353 (1979).
- (7) (a) M. Stock and H. Yersin, *Chem. Phys. Lett.*, **40**, 423 (1976); (b) M. Stock and H. Yersin, *Solid State Commun.*, **27**, 1305 (1978).
- (8) H. Yersin, I. Hidvegi, G. Gliemann, and M. Stock, *Phys. Rev. B: Condens. Matter* **19**, 177 (1979).
- (9) (a) G. Gliemann, W. Holzapfel, and H. Yersin, *Ber. Bunsenges. Phys. Chem.*, **82**, 1249 (1978); (b) W. Holzapfel, H. Yersin, and G. Gliemann, *J. Chem. Phys.*, **74**, 2124 (1981); (c) W. Holzapfel, Thesis, University of Regensburg, 1978; (d) R. Schultheiss, I. Hidvegi, and G. Gliemann, to be submitted for publication.
- (10) A. K. Viswanath and H. H. Patterson, *Chem. Phys. Lett.*, **82**, 25 (1981).
- (11) B. G. Anex and R. L. Musselman, *J. Phys. Chem.*, **84**, 883 (1980).
- (12) (a) I. Hidvegi, W. v. Ammon, and G. Gliemann, *J. Chem. Phys.*, **76**, 4361 (1982). (b) I. Hidvegi, Thesis, University of Regensburg, 1982.
- (13) (a) W. v. Ammon and G. Gliemann, *J. Chem. Phys.*, **77**, 2266 (1982); (b) W. v. Ammon, Thesis, University of Regensburg, 1981.
- (14) (a) H. P. Pflieger and K. Krogmann, to be submitted for publication; (b) H. P. Pflieger, Thesis, University of Karlsruhe, 1981.

(15) A. Engl Müller, Diplomarbeit, University of Regensburg, 1981.

(16) H. Yersin and G. Gliemann, *Messtechnik (Braunschweig)*, **80**, 99 (1972).

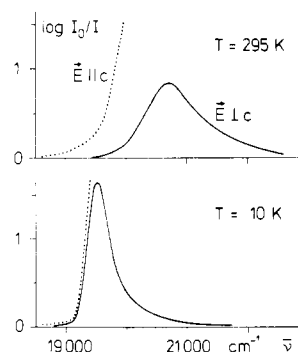


**Figure 1.** Polarized absorption spectra of enH<sub>2</sub>CP at  $T = 295$  K and  $T = 10$  K (thickness of the crystals  $20 \mu\text{m}$ ).

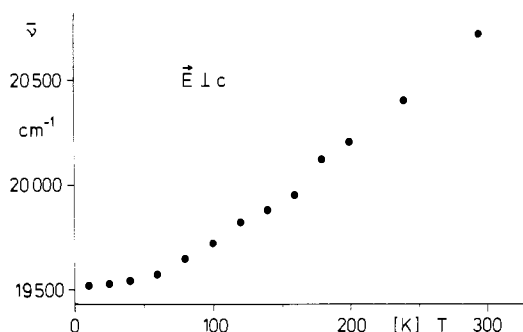


**Figure 2.** Temperature dependence of the  $\vec{E}_{\perp c}$  absorption maximum of enH<sub>2</sub>CP single crystals.

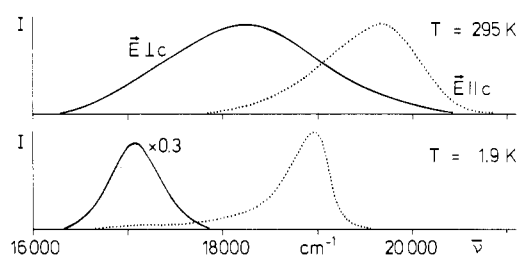


**Figure 3.** Polarized emission spectra of enH<sub>2</sub>CP at  $T = 295$  K and  $T = 1.9$  K ( $\lambda_{\text{ex}} = 364$  nm).

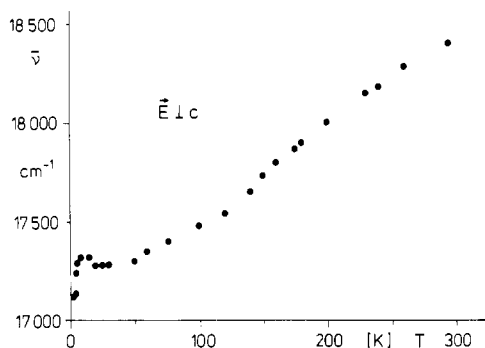


**Figure 4.** Temperature dependence of the  $\vec{E}_{\perp c}$  emission maximum of enH<sub>2</sub>CP single crystals.

temperature range between  $T = 7$  K and  $T = 1.9$  K we observe an additional red shift of about  $230 \text{ cm}^{-1}$ . When the crystals are cooled from  $T \approx 10$  K to  $T = 1.9$  K, the  $\vec{E}_{\perp c}$  emission intensity decreases remarkably.

**Polarized Emission at High Pressure.** enH<sub>2</sub>CP exposed to high hydrostatic pressures shows a drastic red shift of the emission bands (Figure 5). Between  $P = 1$  atm and  $P = 10.5$  kbar we found for the highly energetic  $\vec{E}_{\parallel c}$  emission a gradient  $\Delta\bar{\nu}/\Delta P \approx 360 \text{ cm}^{-1}\cdot\text{kbar}^{-1}$ , the largest value on record in the literature, whereas the  $\vec{E}_{\perp c}$  emission shift amounts to  $260 \text{ cm}^{-1}\cdot\text{kbar}^{-1}$ , similar to the shift observed with MgCP.<sup>7b</sup> In the range between  $P = 10.5$  and  $16$  kbar the emission maxima

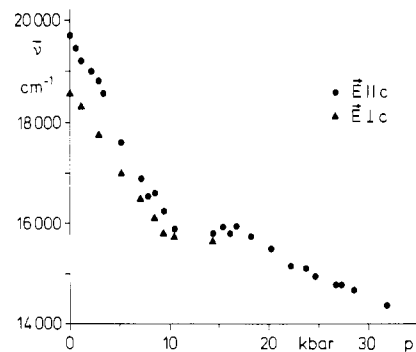


**Figure 5.** Red shift of the polarized emission maxima of enH<sub>2</sub>CP single crystals as a function of hydrostatic pressure ( $\lambda_{\text{ex}} = 364$  nm).

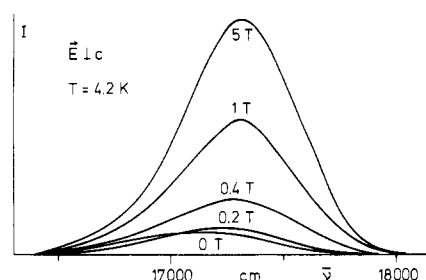


**Figure 6.**  $\vec{E}_{\perp c}$  polarized emission spectra of enH<sub>2</sub>CP at different magnetic field strengths (vector orientation  $\vec{H} \perp \vec{O} \perp c$ ,  $\lambda_{\text{ex}} = 364$  nm).

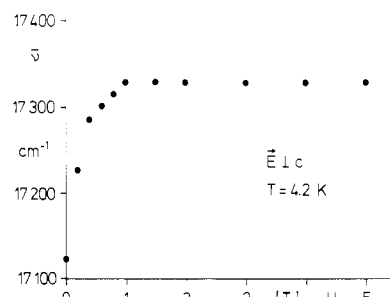


**Figure 7.** Blue shift of the  $\vec{E}_{\perp c}$  polarized emission maximum of enH<sub>2</sub>CP single crystals as a function of magnetic field strength (vector orientation  $\vec{H} \perp \vec{O} \perp c$ ,  $\lambda_{\text{ex}} = 364$  nm).

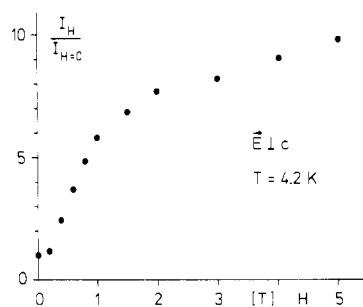


**Figure 8.** Relative intensity of the  $\vec{E}_{\perp c}$  polarized emission of enH<sub>2</sub>CP single crystals as a function of magnetic field strength (vector orientation  $\vec{H} \perp \vec{O} \perp c$ ,  $\lambda_{\text{ex}} = 364$  nm).

are not influenced by pressure variation. Above  $16$  kbar the emission maxima of  $\vec{E}_{\parallel c}$  and  $\vec{E}_{\perp c}$  have nearly the same frequency and were shifted by  $\sim 100 \text{ cm}^{-1}\cdot\text{kbar}^{-1}$  to the red.

With increasing pressure the half-widths of both polarized emissions as well as the intensity ratio of the  $\vec{E}_{\perp c}$  emission and the high-energy  $\vec{E}_{\parallel c}$  emission decrease.

**Polarized Emission at Strong Magnetic Fields.** The behavior of the  $\vec{E}_{\perp c}$  emission under the influence of strong magnetic fields is presented in Figure 6. The measurements were carried out at  $T = 4.2$  K and for the vector orientations  $\vec{H} \perp c$ ,  $\vec{H} \perp \vec{O}$ , and  $\vec{O} \perp c$ , where  $\vec{O}$  denotes the direction of observation

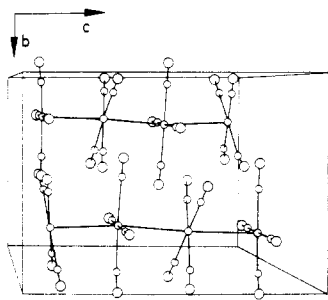


**Figure 9.** Stereoscopic view of the tetracyanoplatinate chains in enH<sub>2</sub>CP (crystallographic orientation [010]).

and  $\vec{H}$  the magnetic field vector.

Figure 7 shows the energy of the  $\vec{E} \perp c$  emission as a function of the magnetic field strength. Between  $H = 0$  and 1 T a large blue shift of  $\sim 220 \text{ cm}^{-1}$  is observed. Above  $H = 1$  T the spectral position of the  $\vec{E} \perp c$  emission remains constant.

Magnetic fields exert a drastic influence on the  $\vec{E} \perp c$  emission intensity (Figure 8). The relative intensity  $I_H/I_{H=0}$  increases between  $H = 0$  and 5 T by a factor of 10. No saturation effect of the intensity growth is found up to 5 T.

The highly energetic  $\vec{E} \parallel c$  emission is not found to be influenced by magnetic fields.

### Discussion

The interpretation of our experimental results will be based on the structural data of the enH<sub>2</sub>CP single crystal. As shown by Krogmann and Pflieger,<sup>14</sup> the [Pt(CN)<sub>4</sub>]<sup>2-</sup> complex ions have nearly  $D_{4h}$  symmetry and are arranged as presented in Figure 9. The columns are parallel and have a quite good linearity with Pt–Pt–Pt angles of 173.8 and 175.9°. Within a column the Pt–Pt distance  $R$  alternates with values of 3.286 and 3.268 Å. For further structural details see ref 14.

This structure encourages us to discuss our results within a model applied in the past to MCP's with inorganic cations.<sup>17</sup> The approximate positions of the electronic states are described by a valence band and a conduction band generated by intrachain coupling of hybrid molecular states, Pt 5d<sub>z<sup>2</sup></sub>, 6s and Pt 6p<sub>z</sub>, CN  $\pi^*$ , respectively. As shown by an appropriate band calculation in the framework of the extended Hückel approximation, the  $R$  dependence of the band gap confirms the  $R^{-3}$  law for the excitation energies as found previously from empirical data.<sup>18</sup>

Starting with the  $R^{-3}$  law (for  $T = 295 \text{ K}$ )<sup>3</sup>

absorption:

$$\vec{E} \perp c \quad \bar{\nu}_{\perp} = 43.9 \times 10^3 - (8.0 \times 10^5)R^{-3}$$

emission:

$$\vec{E} \parallel c \quad \bar{\nu}_{\parallel} = 42.9 \times 10^3 - (8.0 \times 10^5)R^{-3}$$

$$\vec{E} \perp c \quad \bar{\nu}_{\perp} = 36.8 \times 10^3 - (6.3 \times 10^5)R^{-3}$$

with a mean Pt–Pt distance of  $\sim 3.277 \text{ Å}$ , we get the values

absorption:

$$\bar{\nu}_{\perp} = 21\,170 \text{ cm}^{-1} \quad (\bar{\nu}_{\perp}(\text{exptl}) = 20\,720 \text{ cm}^{-1})$$

emission:

$$\bar{\nu}_{\parallel} = 20\,170 \text{ cm}^{-1} \quad (\bar{\nu}_{\parallel}(\text{exptl}) = 19\,760 \text{ cm}^{-1})$$

$$\bar{\nu}_{\perp} = 18\,900 \text{ cm}^{-1} \quad (\bar{\nu}_{\perp}(\text{exptl}) = 18\,350 \text{ cm}^{-1})$$

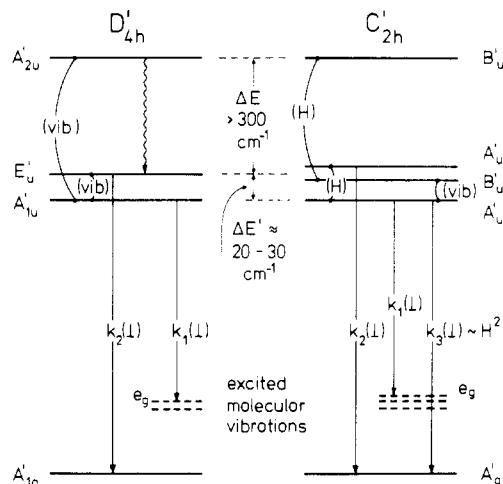


**Figure 10.** Energy level diagrams for the  $\vec{E} \perp c$  emitting states of a [Pt(CN)<sub>4</sub>]<sup>2-</sup> chain: (left side) without magnetic field; (right side) under the influence of a magnetic field (vector orientation  $\vec{H} \perp c$ ).

The deviation between calculated and measured wavenumbers is smaller than 3%.

The observed red shift of the emission with increasing pressure (Figure 5) finds its interpretation by this model, too. The red shift between  $P = 1$  atm and 10.5 kbar corresponds to an  $R$  reduction of  $\sim 0.27 \text{ Å}$ . This extreme compressibility ( $\chi_c \approx 5.3 \times 10^{-3} \text{ kbar}^{-1}$ ) of the enH<sub>2</sub>CP single crystals may be due to the voluminosity structured cations, which can evade the external pressure by a slight rearrangement in the crystal.

Between  $P = 10.5$  and 16 kbar the emission and, therefore, the intracolumnar Pt–Pt distances are constant. We suppose that in this pressure range the crystal undergoes a phase transition. Possibly the gauche enH<sub>2</sub><sup>2+</sup> cation changes into its more common trans conformation. A further indication of a phase transition is given by the fact that above 16 kbar the red shift is linear again but has a drastically smaller  $\Delta\bar{\nu}/\Delta P$  value as is the case below 10.5 kbar.

At high pressures the energy difference between the  $\vec{E} \perp c$  and the  $\vec{E} \parallel c$  emissions becomes somewhat smaller than expected from the  $R^{-3}$  law. The reason for this behavior may be seen in the increase of the intensity ratio  $I_{\parallel}/I_{\perp}$ , which complicates the separation of the two polarization components.

The temperature dependence of the absorption frequency (Figure 2) can be interpreted by the  $R^{-3}$  law. Decreasing temperature is accompanied with a thermal contraction of the intrachain Pt–Pt distance  $R$ . At  $T \approx 50 \text{ K}$  the contraction is practically completed with an  $R$  value of  $\sim 3.20 \text{ Å}$ .

The  $R^{-3}$  law applies analogously to the temperature behavior of the  $\vec{E} \perp c$  emission in the range between room temperature and  $T \approx 10 \text{ K}$ , for this range essentially only one excited state emits with  $\vec{E} \perp c$ , whereas at  $T \lesssim 10 \text{ K}$  at least two excited states are involved, as shown below.

Although the nature of the emitting states is not completely known, recent measurements with doped MCP's<sup>9-11</sup> and magneto-optical studies with MCP's,<sup>12,13</sup> however, have shown that the  $\vec{E} \perp c$  emitting states are arranged at a certain distance below the conduction band. They are strongly localized (probably as self-trapped excitons) and may be approximated by molecular wave functions of the [Pt(CN)<sub>4</sub>]<sup>2-</sup> ion.

A schematically simplified energy level diagram is presented in Figure 10. On the left side we see above the ground state  $A_{1g}'$  the lowest excited energy levels of a [Pt(CN)<sub>4</sub>]<sup>2-</sup> ion, generated by the transition Pt 5d<sub>z<sup>2</sup></sub>, 6s  $\rightarrow$  Pt 6p<sub>z</sub>, CN  $\pi^*$  in  $D_{4h}$  symmetry, with spin-orbit coupling included. A group theoretical analysis predicts electrical dipole-allowed transitions between the  $A_{1g}'$  ground state and the  $A_{2u}'$  and  $E_{u}'$  excited states with polarization  $\vec{E} \parallel c$  and  $\vec{E} \perp c$ , respectively. The

(17) (a) H. Yersin, G. Gliemann, and U. Rössler, *Solid State Commun.*, **21**, 915 (1977); (b) D. W. Bullett, *ibid.*, **27**, 467 (1978); (c) M. H. Whangbo and R. Hoffmann, *J. Am. Chem. Soc.*, **100**, 6093 (1978).

(18) H. Yersin and G. Gliemann, *Ber. Bunsenges. Phys. Chem.*, **79**, 1050 (1975).

transition between  $A_{1u}'$  and  $A_{1g}'$  is symmetry forbidden. Due to electron-phonon coupling, however, there may be relatively weak vibronic transitions from the vibrationally nonexcited  $A_{1u}'$  state to excited vibrational levels of the  $A_{1g}'$  state, namely, an  $\bar{E} \perp c$  transition for an  $e_g$  vibration and an  $\bar{E} \parallel c$  transition for an  $a_{2g}$  vibration.

At low temperatures ( $T \approx 1.9$  K) the sole  $\bar{E} \perp c$  emitting state is the relatively long-lived  $A_{1u}'$ . With increasing temperature  $E_u'$  becomes thermally repopulated and begins to dominate the  $\bar{E} \perp c$  emission, accompanied by a blue shift in the order of the vibrational energy  $e_g$  and an increase of the intensity. This is the explanation of the observed behavior of the  $\bar{E} \perp c$  emission between  $T = 1.9$  and 10 K (Figures 3 and 4).

The right side of Figure 10 presents the energy level diagram of a  $[\text{Pt}(\text{CN})_4]^{2-}$  ion in a homogeneous magnetic field,  $H \perp c$ . The magnetic field lowers the local symmetry to  $C_{2h}'$  and the  $E_u'$  state splits into  $B_u'$  and  $A_u'$ . An important consequence of the symmetry lowering is the magnetic field induced interaction of  $A_u'(E_u')$  and  $A_u'(A_{1u}')$ . This mixing opens up a new radiative channel from the lowest  $A_u$  state to the vibronic  $A_g'$  ground state. This explains the large, magnetically induced blue shift of the  $\bar{E} \perp c$  emission and its saturation behavior at  $T = 4.2$  K when the emission from  $A_u'$  dominates. The observed value of  $220 \text{ cm}^{-1}$  is smaller than the molecular  $e_g$  vibrational wavenumber ( $318 \text{ cm}^{-1}$ ) because the emission from the  $E_u'$  state cannot be totally neglected at  $T = 4.2$  K.

### Conclusion

With  $\text{enH}_2\text{CP}$  for the first time a tetracyanoplatinate(II) complex with an organic cation has been studied by spectroscopic methods. The optical properties (polarized absorption

and emission) of  $\text{enH}_2\text{CP}$  single crystals measured under variation of temperature ( $1.9 \text{ K} \leq T \leq 295 \text{ K}$ ), hydrostatic pressure ( $1 \text{ atm} \leq P \leq 32 \text{ kbar}$ ), and magnetic fields ( $0 \leq H \leq 5 \text{ T}$ ) behave just like those found for tetracyanoplatinates(II) with alkali or alkaline-earth cations. There we see a further strong indication that the role of the cations seems to be restricted to the adjustment of the intrachain Pt-Pt distance  $R$ .

With decreasing temperature down to  $T \approx 50$  K the absorption energy is shifted to the red. Below this temperature it remains constant. A corresponding behavior has been observed for the polarized emission between room temperature and  $T \approx 10$  K. Following the  $R^{-3}$  law, which correlates the optical frequencies of quasi-one-dimensional tetracyanoplatinates(II) with the intrachain Pt-Pt distance  $R$ , the observed temperature dependence expresses a thermal contraction, which is completed at  $T \approx 50$  K. The polarized emission of  $\text{enH}_2\text{CP}$  single crystals shows a drastic pressure-induced red shift of  $\sim 360 \text{ cm}^{-1} \cdot \text{kbar}^{-1}$ , corresponding to a linear compressibility of  $\sim 5.3 \times 10^{-3} \text{ kbar}^{-1}$ . Above 10.5 kbar the crystals seem to undergo a phase transition.

In the low-temperature range between  $T = 1.9$  K and  $T \approx 10$  K at least two excited states take part in the  $\bar{E} \perp c$  emission. Below  $T \approx 5$  K the upper one is frozen out. Increasing the temperature and raising the magnetic field strength  $H \perp c$  yields a blue shift of  $\sim 220 \text{ cm}^{-1}$ , which is traced back to a vibrational quantum of the crystal-bound  $[\text{Pt}(\text{CN})_4]^{2-}$  ion.

**Acknowledgment.** The authors are greatly indebted to I. Hidvegi, A. Englmüller, and R. Schultheiss for valuable discussions. The "Verband der Chemischen Industrie" is acknowledged for financial support.

Registry No.  $\text{enH}_2\text{CP}$ , 84927-45-7.

Contribution from the Radiation Laboratory,  
University of Notre Dame, Notre Dame, Indiana 46556

## Photochemistry of Transition-Metal Phthalocyanines. Analysis of the Photochemical and Photophysical Properties of the Acido(phthalocyaninato)rhodium(III) Complexes

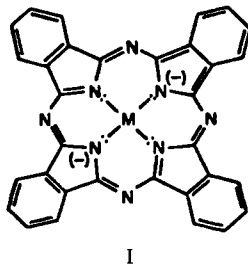
G. FERRAUDI\* and S. MURALIDHARAN

Received May 28, 1982

The ultraviolet photochemistry of the rhodium(III) phthalocyanines  $\text{Rh}(\text{ph})(\text{CH}_3\text{OH})\text{X}$  with  $\text{X} = \text{Cl}^-$ ,  $\text{Br}^-$ , and  $\text{I}^-$  was investigated at different wavelengths. The same action spectrum for the photoinduced hydrogen abstraction was obtained for the three compounds. The photonic energy of the excitation is degraded in part by emission at short wavelengths, e.g.  $\lambda_{\text{max}} \approx 420 \text{ nm}$ . Such a violet emission, observed with phthalocyanines of Al(III), Rh(III), Co(III), and Ru(II), has been attributed to the relaxation of an upper  ${}^3\pi\pi^*$  excited state. The emission spectra at 77 K exhibited vibronic components with a separation between successive peaks  $\Delta\nu \approx 1.3 \times 10^3 \text{ cm}^{-1}$ . A comparison between the excitation and action spectra shows the difference in the paths that populate the reactive  $n\pi^*$  and upper emissive  $\pi\pi^*$  states. An investigation of the time dependence of the upper  ${}^3\pi\pi^*$  emission and lowest  ${}^3\pi\pi^*$  absorptions reveals the participation of triplet sublevels in the degradation of the excitation energy. The relationship between photoemissive and photoreactive states is discussed.

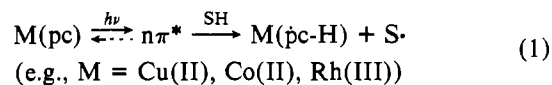
### Introduction

The ultraviolet photochemistry of several monomeric and dimeric transition-metal phthalocyanines (I) has been inves-



tigated in recent years.<sup>1-6</sup> Most of these compounds undergo

photoinduced reductions by abstraction of hydrogen from the solvent (eq 1). Such a photochemical reactivity has been



associated with the population of reactive  $n\pi^*$  excited states,

- (1) G. Ferraudi and E. V. Srisankar, *Inorg. Chem.*, **17**, 3164 (1978).
- (2) G. Ferraudi, *Inorg. Chem.*, **18**, 1005 (1979).
- (3) K. Schmatz, S. Muralidharan, K. Madden, R. Fessenden, and G. Ferraudi, *Inorg. Chim. Acta*, **64**, L23 (1981).
- (4) R. Prasad and G. Ferraudi, *Inorg. Chim. Acta*, **54**, L231 (1981).
- (5) R. Prasad and G. Ferraudi, *Inorg. Chem.*, **21**, 2967 (1982).
- (6) K. Schmatz, S. Muralidharan, and G. Ferraudi, *Inorg. Chem.*, **21**, 2961 (1982).